Journal of Thermal Engineering
Yildiz Technical University Press, Istanbul, Turkey
Vol. 2, Special Issue 4, No. 4, pp. 882-896, July, 2016.

http://eds.yildiz.edu.tr/journal-of-thermal-engineering/Articles
Manuscript Received September 09, 2015; Accepted December 03, 2015

This paper was recommended for publication in revised form by Regional Editor Balaram Kundu

EFFECTS OF PARTIAL HEATING OF TOP ROTATING LID WITH AXIAL TEMPERATURE GRADIENT ON VORTEX BREAKDOWN IN CASE OF AXISYMMETRIC STRATIFIED LID DRIVEN SWIRLING FLOW

Subas Chandra Dash
Research scholar, Aerospace Engineering Department, IIT Kharagpur.
West Bengal ,India

N. Singh
Professor, Aerospace Engineering Department, IIT Kharagpur.
West Bengal ,India

Key words: Stratified fluid, partial Heating, lid driven swirling flow, axisymmetric.
** Corresponding author:, Phone: (91) 7725863514*
E-mail address: subasiitkgp@gmail.com

ABSTRACT

The present numerical simulation investigates the effects of partial heating on confined stratified swirling flow in a cylindrical cavity with a top rotating lid. The flow patterns and the heat transfer characteristics are numerically investigated under the Boussinesq assumptions. The inner region of the surface of top rotating lid of cylindrical cavity, with radius less than or equal to radius of the lid, is kept at a higher temperature as compared to the bottom stationary wall. The remaining outer region of the top rotating lid and the side wall are perfectly insulated. A systematic study has been carried out by varying radius of the hotter region of the top rotating lid. Steady state axisymmetric solutions are obtained in cylindrical regime with a fixed values of the governing parameters, the Reynolds number 1500, Richardson number 0.05 and Prandtl number 1.0 for a cavity of aspect ratio 1.8. The vortex breakdown size, numbers and position are found to be changing with increase in partial heating. Variation in magnitude of local as well as average Nusselt number in vicinity to top rotating lid are significantly influenced by increase in partial heating radius of top rotating lid. Also variations in coefficient of torque are studied.

INTRODUCTION

The confined swirling or rotating flows in a cylindrical cavity , developed by constantly rotating one of the top or bottom discs, are invetigated by the pioneering works of Vogel[1],Pao[2], Bertela and Gori[3] and Lugt and Haussling[4]. The same study has been systematically carried out experimentally by Escuder[5] by means of fluorescent dye visualisation technique. He has developed from experiment zones of of single,double,and tripple axisymmetic vortex breakdown in AR-Re(aspect ratio and Reynold number) plane within the axis of rotation in steady state flow region.The vortex breakdown behaviors have been verified by Lugt, &Abboud[6] in their study of Axisymmetric vortex breakdown with and without temperature effects in a container with arotating lid. They have investigated the effects of Prandtl number, Richardson number, Reynolds number and Eckert Number on the behavior of swirling flow and vortex breakdown under the natural, forced and mixed convection conditions. The thermal effects on vortex breakdown has been studied in a confined rotating concentric spherical annulus by Arkadyev et al.[7]. The flow field show various types of flow patterns and vortex breakdown: bubble type vortex breakdown, a vortex ring, or development of recirculation zone.Such changes in flow phenomenas are related with the geometry of spherical gap of container and on the relative strength of the imposed temperature difference and rate of rotation.

The behavior of vortex breakdown for very low and high Prandtl number ,under the influence of gravitationally stable and unstable situation, in the cylindrical geometry is studied by Lee and Hyun[8].Kim and Hyun[9] have discussed the intensification of internal flow within the cylindrical cavity and resulting increase in convectively controlled heat transfer in the fluid with the help of axial temperature gradient. The interest of their study is the behaviours of vortex breakdown bubble ,and the attendant heat transfer under the influence of stable stratification.The computed local Nusselt number ,at top and bottom discs, invetigates its augmention which is controled by convective heat transfer is discussed in their computation for cylinder with aspect ratio of 2.0.

R. Iwatsu[10] has investigated confined swirling flow where the temperature of the top disc is maintained higher than that of the bottom disc.However, his computation obiective has been to obtaining the behavior of the flow at moderated value of Richardson number and gatther information on its effects on calculated average Nusslet number and average coefficient of torque. R. Iwatsu[10] has also discovered that meridional secondary flow reveals flow separation on the lower boundary as well as on the axis depending on the values of Ri and Re.His conclusion is that the average Nusselt number $\overline{Nuav}$ and the torque coefficient $CTorq$ are computaed as function of Re and Ri.Chen[11] first time investigated entropy generation inside lid driven rotating convensional flow.In his flow model he uses a rotating lid having radius less than the radius of cylindrical cavity. This small rotaing lid is kept at higher temprature with respect to the lower fixed wall. He discussed, the effects of rotating of this disk, described by the Reynolds number and the buoancy force described by Grashof number, on entropy generation considering systematically the situtation of the forced convection,natural convection and mixed convection.

The present work involves study of the behavior of vortex breakdown in thecase of partial heating of top rotating lid for stratified fluid or Boussinesq fluid in presence of axial heat flux. The inner region of the surface of top rotating lid of cylindrical cavity, with radius less than or equal to radius of the lid, is kept at a higher temperature as compared to the bottom stationary wall. The remaining outer region of the top rotating lid and the side wall are perfectly insulated.

A systematic study has been carried out by varying radius of the hotter region of the top rotating lid. Steady state axisymmetric solutions are obtained in cylindrical regime with fixed values of the governing parameters, the Reynolds number 1500, Richardson number 0.05 and Prandtl number 1.0 for a cavity of aspect ratio 1.8.

MATHEMATICALLY FORMULATION

The swirling flow is generated by rotating disk or lid at the top of the cylindrical cavity, filled with viscous stratified fluid, with constant angular velocity. The inner region of the surface of top rotating lid of cylindrical cavity is kept at a higher temperature as compared to the bottom stationary wall as shown in red color in Fig.1. A stable temperature gradient is maintained, between the partial top rotating lid and the bottom fixed wall, in axial direction in order to investigate the effects of heat transfer upon the swirling flow pattern and vortex breakdown as shown in Fig 1.

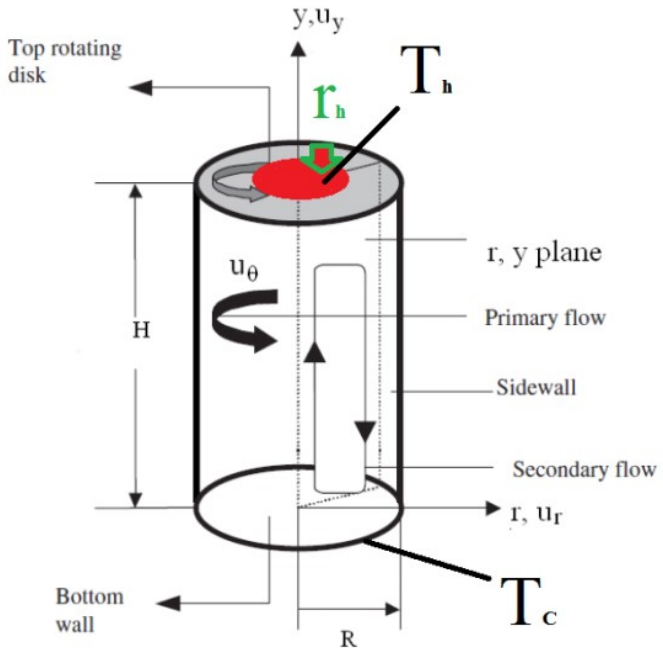

Fig. 1 Schematic illustration of cylindrical domain with parameters in case of partial heating

Governing Equations

In the cylindrical coordinate systems $[u_r, u_\theta, u_y]$ are the velocity components in $[r, \theta, y]$ directions respectively. For two dimensional axis-symmetric flows, the dimensionless governing equations in conservative form can be written in cylindrical coordinate system as: Continuity Equation:

$$\frac{1}{r}\frac{\partial(ru_r)}{\partial r}+\frac{\partial u_y}{\partial y}=0 \qquad (1)$$

Momentum equation in radial direction

$$\frac{\partial u_r}{\partial t}+\frac{1}{r}\frac{\partial(ru_ru_r)}{\partial r}+\frac{\partial(u_ru_y)}{\partial y}-\frac{u^2{}_\theta}{r}= -\frac{\partial p}{\partial r}+\frac{1}{\mathrm{Re}}\left[\frac{\partial^2 u_r}{\partial r^2}+\frac{1}{r}\frac{\partial u_r}{\partial r}+\frac{\partial^2 u_r}{\partial y^2}-\frac{u_r}{r^2}\right] \qquad (2)$$

Momentum equation in axial direction

$$\frac{\partial u_y}{\partial t}+\frac{1}{r}\frac{\partial\left(ru_r u_y\right)}{\partial r}+\frac{\partial\left(u_y u_y\right)}{\partial y^*}=-\frac{\partial p}{\partial y}$$
$$+\frac{1}{\mathrm{Re}}\left[\frac{\partial^2 u_y}{\partial r^2}+\frac{1}{r}\frac{\partial u_y}{\partial r}+\frac{\partial^2 u_y}{\partial y^2}\right]+RiT \quad (3)$$

Momentum Equation in azimuthal direction:

$$\frac{\partial u_\theta}{\partial t}+\frac{1}{r}\frac{\partial\left(ru_r u_\theta\right)}{\partial r}+\frac{\partial\left(u_y u_\theta\right)}{\partial y}-\frac{u_r u_\theta}{r}=$$
$$\frac{1}{\mathrm{Re}}\left[\frac{\partial^2 u_\theta}{\partial r^2}+\frac{1}{r}\frac{\partial u_\theta}{\partial r}+\frac{\partial^2 u_\theta}{\partial y^2}-\frac{u_\theta}{r^2}\right] \quad (4)$$

Energy Equation:

$$\frac{\partial T}{\partial t}+u\frac{\partial T}{\partial r}+v\frac{\partial T}{\partial y}=$$
$$\frac{1}{\mathrm{Re}\,\mathrm{Pr}}\left(\frac{1}{r}\frac{\partial}{\partial r}\left(r\frac{\partial T}{\partial r}\right)+\left(\frac{\partial^2 T}{\partial y^2}\right)\right) \quad (5)$$

where the reference scale for length, time, velocity and pressure are R,Ω^{-1}, $R\Omega$ and $\rho R^2\Omega^2$ respectively. The temperature T Ta is non-dimensionalized as $T=\frac{T-T_C}{T_h-T_C}$.

where T_h & T_C are temperatures at known lower cooler & upper hotter disk (partial) respectively. The remaining outer region of the top rotating lid and the side wall are perfectly insulatedthermally. The parameters which govern the fluid motion and temperature distribution and are used in the present study are defined:

Reynolds number: $\mathrm{Re}=\frac{\Omega R^2}{\nu}$ where ν is the kinematic viscosity.

Richardson Number: $Ri=\frac{g\beta(T_h-T_C)}{\Omega^2 R}$ where g- acceleration due to gravity, β - thermal expansion coefficient of fluid.The magnitude of Ri Richardson number decides the type of convection during the flow process. Prandtl number: $\mathrm{Pr}=\frac{\nu}{\alpha}$, where α is the thermal diffusivity

Hydrodynamic boundary conditions

$$r=0,0\le y\le h,u_r=0,u_\theta=0,\frac{\partial u_y}{\partial r}=0$$
$$r=1,0\le y\le h,u_r=0,u_\theta=0,u_y=0$$
$$y=0,0\le r\le 1,u_r=0,u_\theta=0,u_y=0$$
$$y=h,0\le r\le 1,u_r=0,u_\theta=\Omega\times r,u_y=0 \quad (6)$$

Thermal boundary condition

$$r=0,\le y\le h,\frac{\partial T}{\partial r}=0 \quad r=1.0,0\le y\le h,\frac{\partial T}{\partial r}=0$$
$$y=0,0\le r\le 1,T=0 \quad y=h,0\le r\le r_h,T=1$$
$$y=h,r_h\le r\le 1,\frac{\partial T}{\partial r}=0 \quad (7)$$

The convective terms in the momentum equations are discretized by central/upwind differencing whereas the viscous terms are always approximated by second order central differencing. Pressure terms are also discretized using central differencing. In case of energy equation both the convection as well as the heat conduction terms are approximated using central differencing.

NUMERİCAL METHOD OF SOLUTION

In the staggered grid arrangement various physical quantities are stored at different location in a cell as shown in Fig.1.2. In the cylindrical coordinate systems u_r,u_θ,u_y are the velocities in r,θ,y directions respectively. The governing equations are solved by finite difference method. In the present scheme the scalar quantities (p; T) are stored at the centre of the cell, whereas the velocity components of the velocity vector u_r,u_y are stored on the cell faces. However, for axisymmetrc case velocity component u_θ is also stored at the cell centre.

Knowing the solution at nth time level u_r,u_θ,u_y, p, T the aim is to obtain the solution at next time level. The procedure of solving radial and axial momentum equations is based on pressure correction technique and subsequently finite difference solution of angular momentum equation is obtained. While advancing solution from nth time to (n+1)th level explicitly one get velocity field which may or may not satisfy

the continuity equation. This problem is resolved by using pressure correction technique where the pressure and velocity components for each cell are corrected iteratively in such a way that for the final pressure field the velocity divergence in each cell vanishes. The iterative process is continued till the velocity divergence for each cell is less than the prescribed upper limit, for the present study it has been taken as 0.000001. Finally the velocity boundary conditions are also corrected and one gets a divergence free converged velocity field, at $(n+1)^{th}$ time level, in all the cells, including the cells at the boundary.

The typical features of pressure correction technique, also referred as modified MAC method, are available in detail in a paper by Chorin [12] and Peyter and Taylor [13] for the solution of incompressible Navier-Stoke equation in rectangular

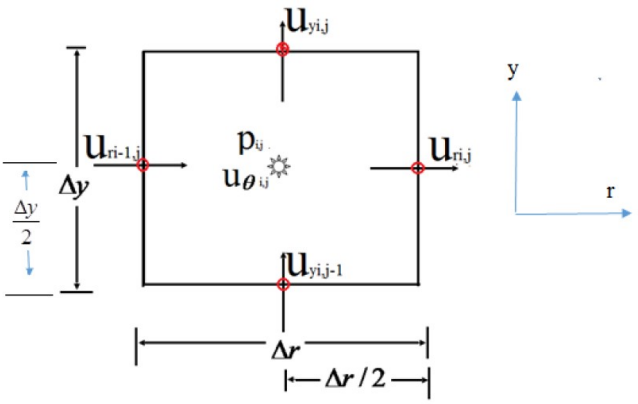

Cartesian co-ordinate system.

After obtaining the corrected radial and axial velocity field using the above pressure correction technique, these velocity components are used to solve the azimuthal momentum equation explicitly to get the $u_{\theta i,j}^{n+1}$ at $(n + 1)^{th}$ time level . The axial momentum equation Eq. 3 involves the temperature T on the right hand side which is known from the n^{th} time level. Once the velocity field is known at $(n+1)^{th}$ time level, the energy equation , Eq`5, is distcritized and solved explicitly.The computation continues till the time one gets steady state solution, if available, or for prescribed number of time steps for unsteady flows. The detail of numerical technique for solution of incompressible Navier-Stoke equation in cylindrical co-ordinate is given in Chapter-3 PhD thesis of Dash [14].

The Solution Procedure

1. The momentum equations along radial and axial directions are solved following the pressure correction technique.

2. After the corrected radial and axialvelocities components are known, momentumequation for azimuthal direction is solved to obtain u_θ .

3. Subsequently the explicit finite difference solution of energy equation, Eq 5, is obtained for temperature field T.

4. Step (1) to step (3) are repeated until convergence for the case where the steady state exits or for a required time for unsteadyflow calculations.

Code Validation

Result for 1.0 Aspect ratio cavity at Reynolds number Re =300, Prandtl number Pr =1.0 and Richardson number Ri =0 show good comparison with the simulated results due to R. Iwatsu(2004) as shown in Fig 3. The axial profiles of present results of radial and azimuthal velocity components at radius r = 0.8 match well with those due to R.Iwatsu (2004). Table 2 shows the results of R.Iwatsu(2004) with three different unequal spacing grids indicating the variation in magnitude of ψ_{max} , ψ_{min} and coefficient of torque. Table -3 shows the present solution with three different equal spacing grids. These tabulated values only reflect the overall similarity of the trends and does not intend to show any comparison because of drastically different grids used in the two studies.

Table 2 R. Iwatsu (2004) at Re=1000,Ri =0.0,Pr=1.0,AR =1.0)

Un-equal spacing grid	R.IWATSU [2004] ψ_{max}	R.IWATSU [2004] ψ_{min}	Co-efficient torque
41X41	$9.96X10^{-3}$	$2.51X10^{-7}$	11.2
81X81	$9.71X10^{-3}$	$1.59X10^{-7}$	11.9
161X 161	$9.64X10^{-3}$	$1.29X10^{-7}$	12.8

Table 3 Present result at Re=1000, Ri =0.0, Pr=1.0, AR =1.0)

Present study	Present- ψ_{max}	Present - ψ_{min}	Coefficient torque
101X101	$9.384X10^{-3}$	$1.683X10^{-7}$	10.060
121X121	$9.395X10^{-3}$	$1.652X10^{-7}$	10.297
151X151	$9.411X10^{-3}$	$1.643X10^{-7}$	10.587

The present result also validated with that due to R. Iwatsu [2015]. The axial profile of radial component of velocity at radius r =0.8, Re =300, Pr =1.0, Ri =0, AR =1.0 is well matched with R. Iwatsu [2015] as shown in Fig 3.

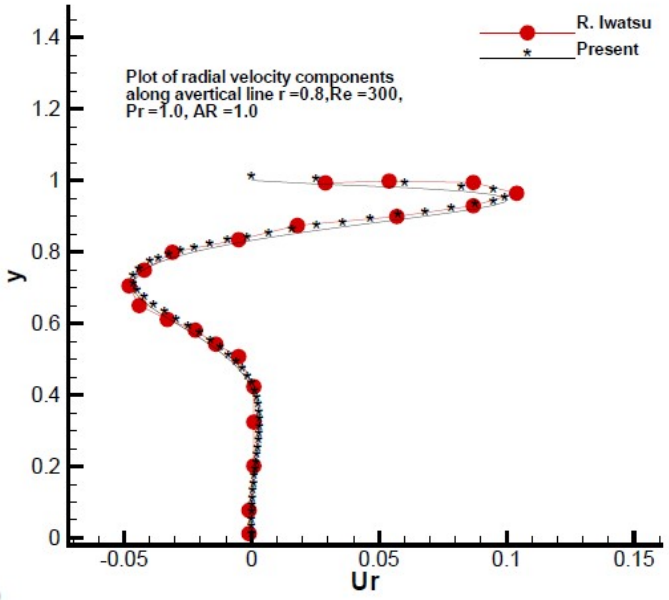

Fig. 3 Axial component of (a) Radial velocity at radius r =0.8, Re =300, Pr =1.0, Ri =0, AR =1.0

RESULTS AND DISCUSSIONS

Nusselt number: at bottom wall $Nu_C = \left.\frac{\partial T}{\partial y}\right|_{y=0}$, at top rotating lid $Nu_h = \left.\frac{\partial T}{\partial y}\right|_{y=0}$, Average Nusselt number: at bottom wall $= \overline{Nu}_C = \frac{1}{\pi}\int_0^1 Nu_C(r)2\pi dr$, Average Nusselt number at top rotating lid $= \overline{Nu}hav = \frac{1}{\pi}\int_0^1 Nu_h(r)2\pi dr$ are computed to investigate the heat convection and conduction property. The coefficient of torque vicinity to top rotating lid $CTtop = \frac{1}{\pi}\int \left.\frac{\partial u_\theta}{\partial y}\right|_{y=h} 2\pi r^2 dr$ is calculated to study the effects of increases in partial heating radius (area) on the primary flow in azimuthal direction i.e. on Ekman boundary layer zone.

Effects of Partial Heating

To investigate the effects of partial heating a lid driven swirling flow in a 1.8 Aspect ratio cavity is considered under the influence of axial temperature gradient. Partial heating is achieved by considering only the inner region of the surface of top rotating lid of cylindrical cavity, with radius less than or equal to radius of the lid, is kept at a higher temperature as compared to the bottom stationary wall. The remaining outer region of the top rotating lid and the side wall are perfectly insulated. This study is carried over with Re =1500, Ri = 0.05 and Prandtl number Pr =1.0.

To understand the effects of partial heating r_h has been varied from 0.0 to 1. The case with r_h=0.0 corresponds to situation where there is no heat transfer and hence a non-stratified fluid motion due to rotation of the top lid. It produces a radial outward flow in the immediate vicinity of the top disk. The fluid then turns downwards near the inner vertical surface of cylinder which again at intermediate radii directed toward the top disk. This produces a clockwise circulation cell in much of interior region of the cylinder and also vortex break down bubble is formed along the axis at around y=0.65 as seen in Fig 4(a). Even with very small partial heating radius r_h =0.2, the convection heat flow starts which slightly influences the size of the vortex breakdown, Fig 4(b). .

The influence of partial heating on vortex break bubble is shown, for different values of radius r_h i.e.is with varying hotter region of top rotating lid, in Fig 4 and Fig 5.When the heating surface area increases the bouncy effect also increases and hence with increase in heat transfer the thermal diffusivity pre-dominates the momentum diffusivity. When r_h is changed from 0.0 to r_h =0.2, both the energy equation (Heat flow) and momentum equation (flow velocity) starts affecting each other. As the flow stratified the thermal diffusivity and momentum diffusivity starts affecting the vortex breakdown shown in Fig: 4 (b). However, the flow has not changed its path significantly. As the partial heating radius (heated area) is further increased from r_h =0.2 to r_h =0.3 and then 0.35 drastic changes have been observed in vortex breakdown separation which can be seen from Fig 4 (c) to Fig 4 (d).

At partial surface heating radius $r_h = 0.35$ two vortex breakdowns starts appearing, one along the axis and another near the axis and vicinity to the bottom fixed wall. At $r_h = 0.37$ vortex breakdowns starts moving downward as shown in Fig 4(e). With further increase in partial heating radius (heated area) the effects of buoyancy effects become more predominant in nature and the vortex in vicinity to the axis starts diffusing .At the same time the lower vortex breakdown i.e. in vicinity to the bottom wall starts enlarging as shown in Fig 4(f) at $r_h = 0.4$. Further increase in heating radius beyond $r_h = 0.4$, a recirculating zone appears in vicinity to

the colder bottom fixed wall along with the circulating zone centered near the top rotating wall. Such phenomena are developed because of increase in convective heat transfer from the top rotating lid and overall temperature gradient increases between the top and bottom wall. The re-circulating zone area near bottom wall increases with increase in partial heating surface beyond $r_h = 0.4$ whereas the upper circulating zone area decreases shown in Fig 5.

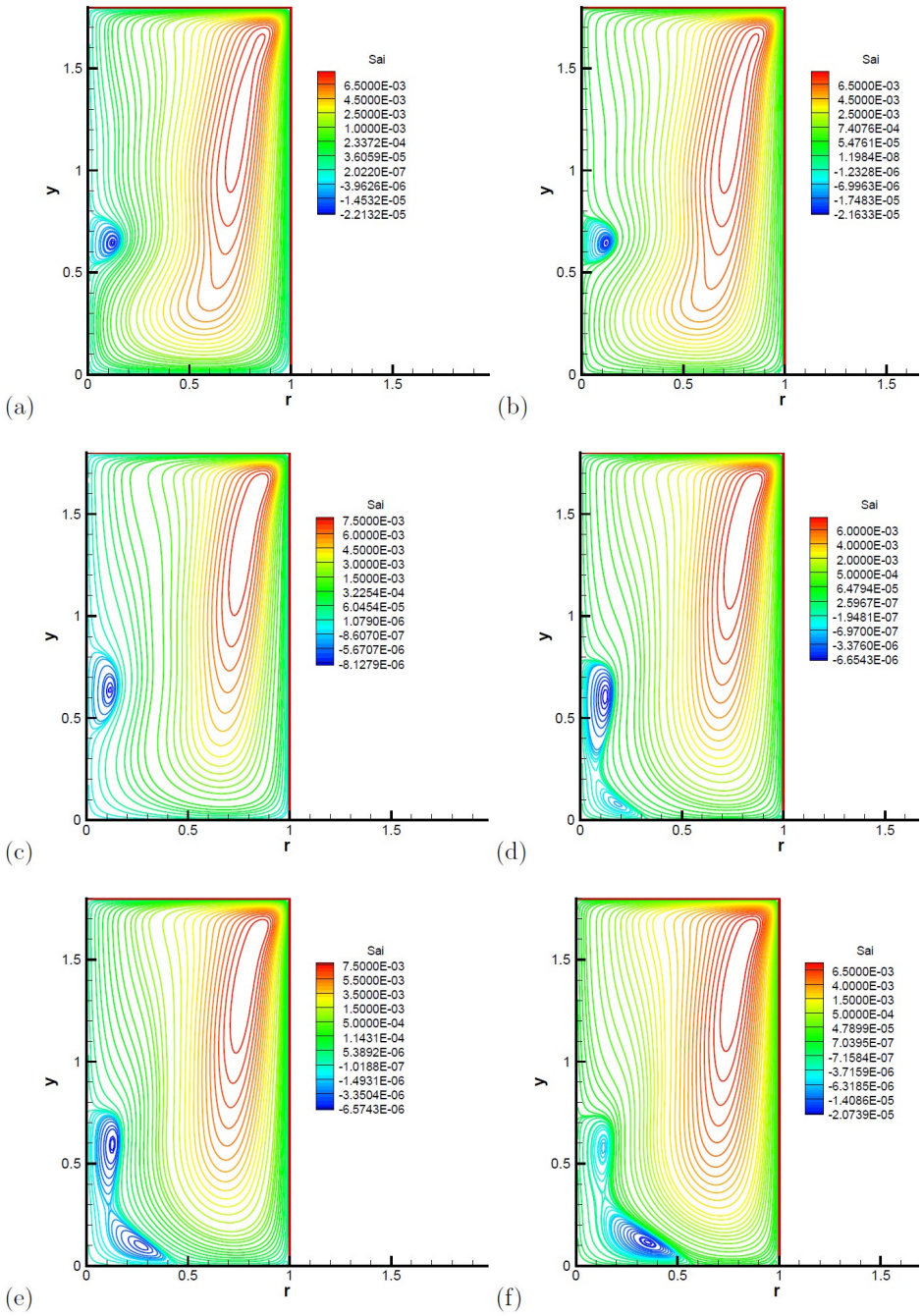

Fig. 4 Contours of steam function at Re= 1500, AR =1.8, Ri =0.05, Pr =1.0.(a) r_h= 0 (b) r_h= 0.2(c) r_h= 0.3(d) r_h= 0.35(e)r_h= 0.37(f) r=0.4

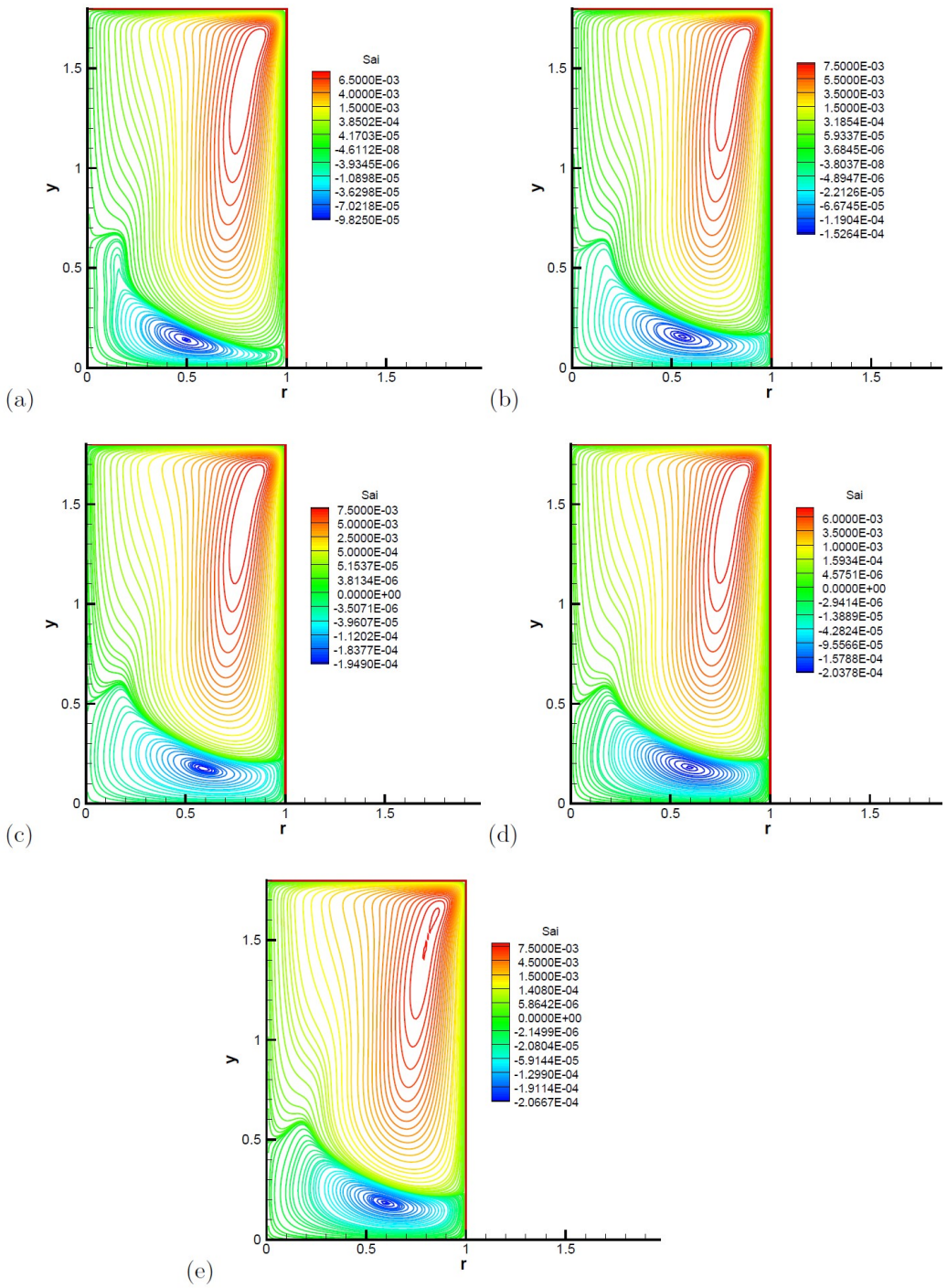

Fig. 5 Contours of steam functionat Re= 1500, AR =1.8,Ri =0.05, Pr =1.0. (a) r_h= 0.5 (b) r_h= 0.6(c) r_h= 0.7(d)r_h= 0.8(e)r_h= 0.9(f)r_h= 1.0

The qualitative change in the meridional flow appears as partial heating radius (area) increases. The relative impact of this stabilizing buoyancy effects is characterized by Richardson number. As shown in Fig 5 the principal changes brought forth by imposing more heating surface area and main circulation is reduced. Under the prevailing stable stratification, the vortex breakdown phenomena's are suppressed.

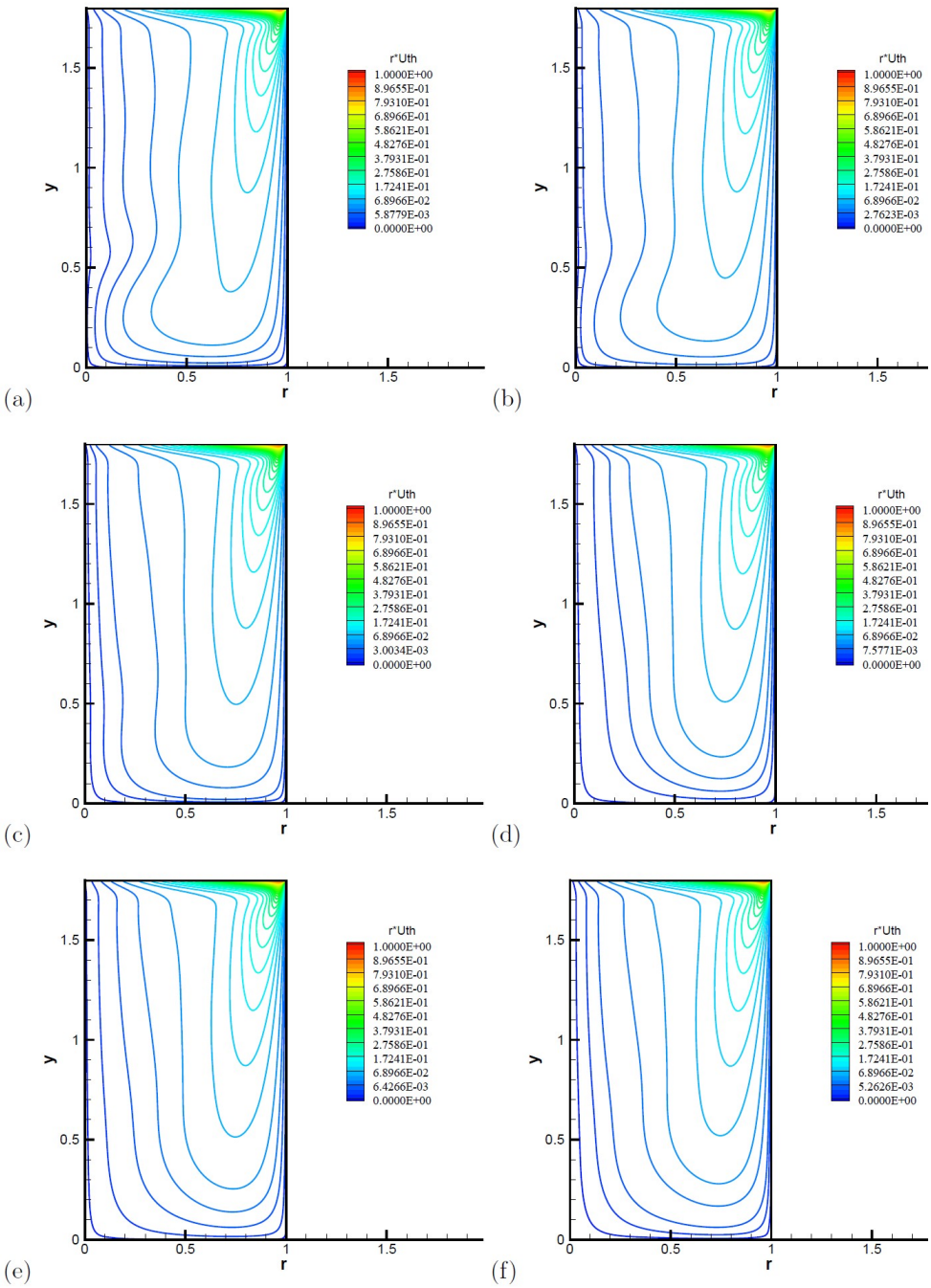

Fig. 6 Contours of angular velocity at Re= 1500, AR =1.8, Pr =1.0.(a) Ri =0.05, r_h= 0 and at Ri =0.05 (b) r_h= 0.2(c) r_h= 0.3(d) r_h= 0.35 (e) r_h= 0.37(f) r_h= 0.

These features are investigative of the meridional flows, particularly the vertical velocity in the core by stabilizing the influence of buoyancy $\Delta T > 0$ However, in negative buoyancy ($\Delta T < 0$) the bubbles becomes larger as stated by Lugt and Abboud(1987) and with increase in absolute value of (Ri).

The contours of azimuthal component of velocity shown in Fig 6(b) to Fig 6(f) and in Fig7 (a) to Fig7 (e) for different partial heating radius at Re =1500, Ri =0.05, Pr =1.0 at aspect ratio AR =1.8.In absence of heating the contours of azimuthal velocity shown in Fig 6(a).

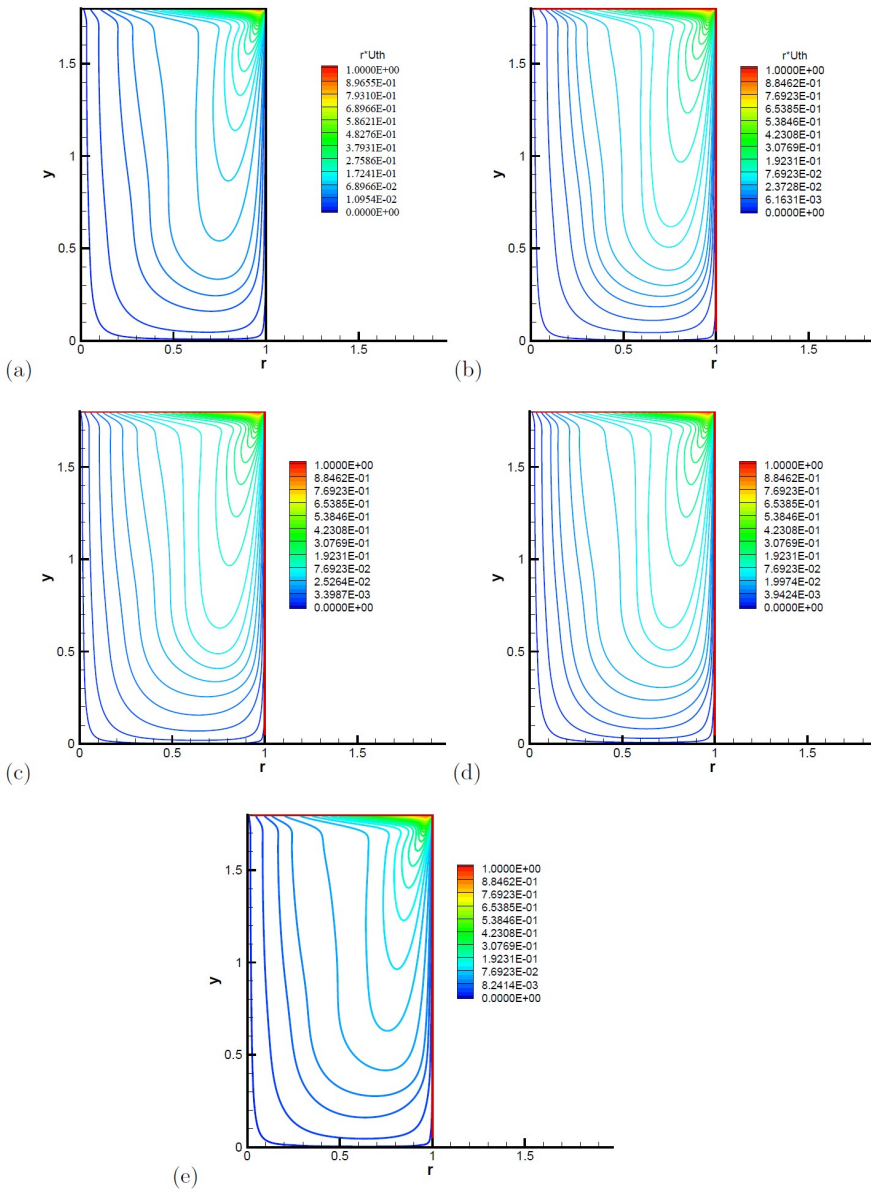

Fig. 7 Contours of angular velocity at Re= 1500, AR =1.8, Pr =1.0,Ri =0.05 (a) r_h= 0.5 (b)r_h =0.6 (c) r_h =0.8 (d) r_h= 0.9 (e)r_h= 1.0

Consequently the azimuthal component of velocity contours lines become straight and vertical in the core with increases in partial heating radius. The gradient of azimuthal velocity in vertical direction reduced in the core region of cavity as shown in Fig 7(a) to Fig7(c) for partial heating radius $r_h = 0.37, r_h = 0.4,\ r_h = 0.5$ .The isotherms contours as shown in Fig 8(b) at Ri =0.05 at small partial heating radius (surface) conduction dominates and isotherms in the core region mostly horizontal. Outside of the core convection heat is dominating and isotherms tend to vertical.

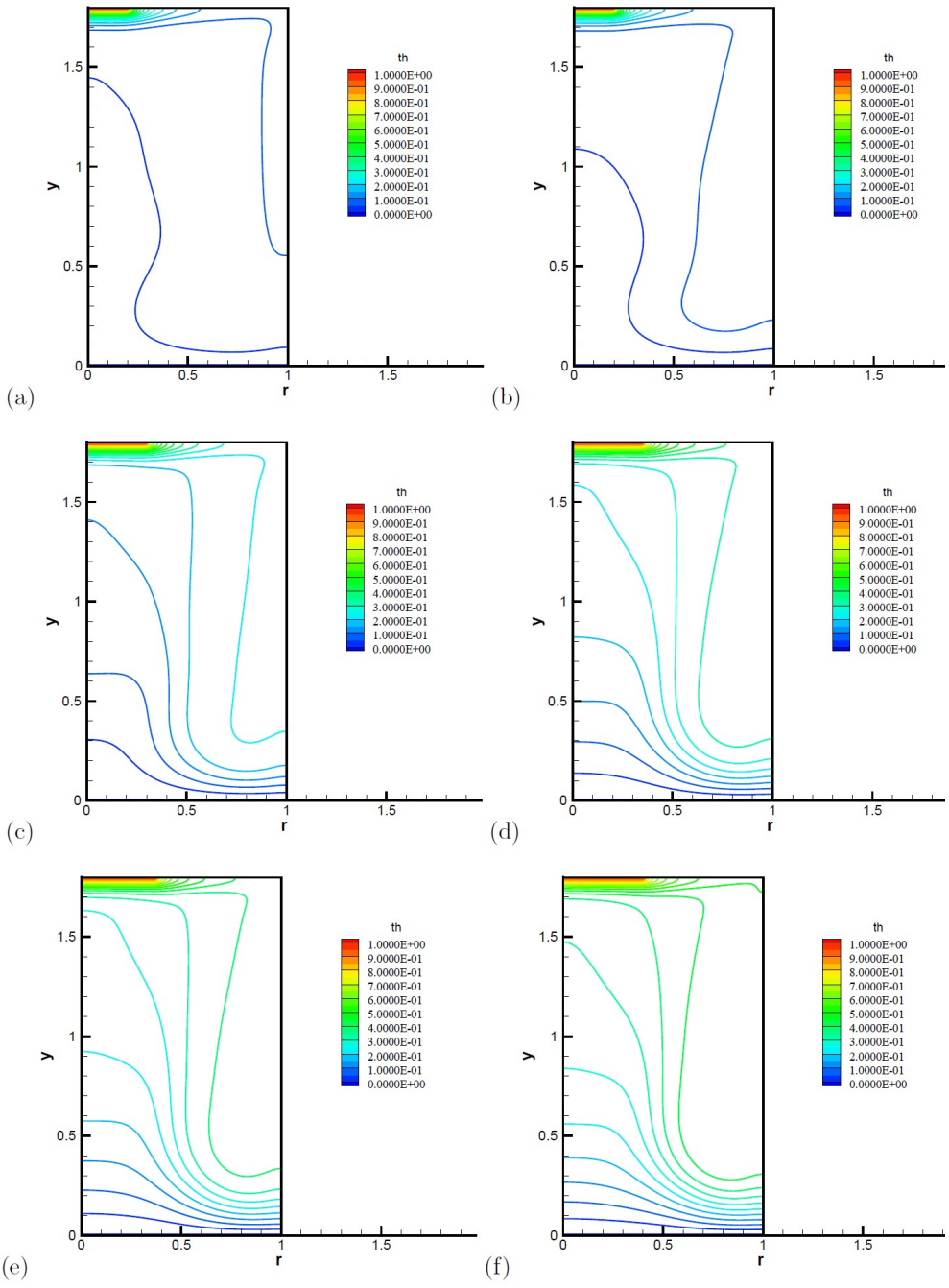

Fig. 8 Contours of isotherms at Re= 1500, AR =1.8, Ri =0.05, Pr =1.0.(a) r_h= 0 (b) r_h= 0.2(c) r_h= 0.3(d) r_h= 0.35.

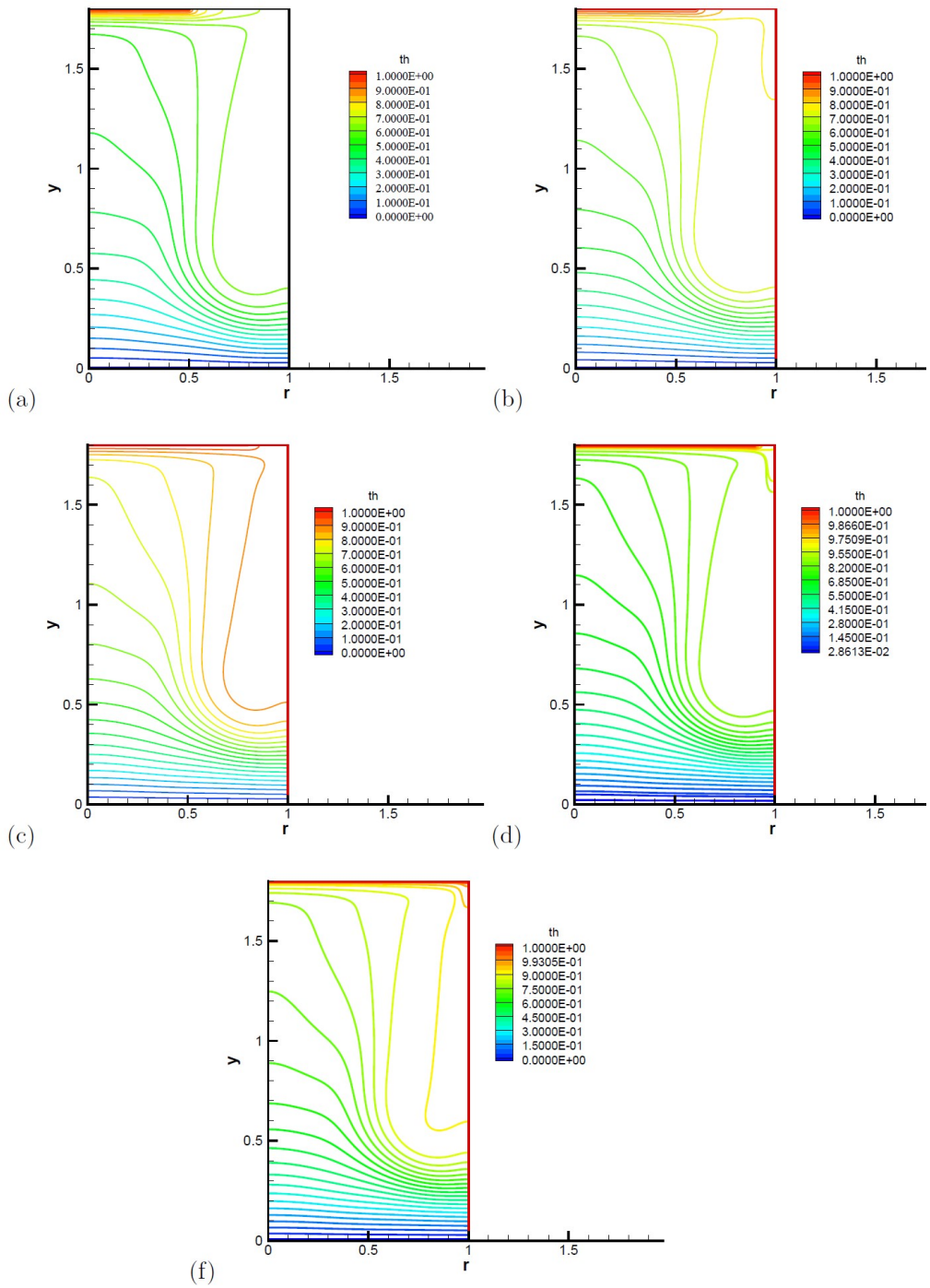

Fig. 9 Contours of isotherms at Re= 1500, AR =1.8,Ri =0.05, Pr =1.0. (a) r_h= 0.5 (b) r_h= 0.6(c) r_h= 0.7(d)r_h= 0.8(e)r_h= 0.9(f)r_h= 1.0

As partial heating radius (surface) increases Convection dominates in most part of the core except vicinity to top and bottom wall as shown in Fig 8(c) to Fig8 (f) .However, with further increase in partial heating surface ($r_h \geq 0.37$) of top rotating lid vertical temperature gradient zones increases near to bottom stationary cold wall. Isotherms become horizontal near to it as shown in Fig 9(a) to Fig 9(e). This proves that the conduction increases near bottom wall with increase in partial heating surface (radius r_h) of top rotating lid. The temperature field also creates a thermal boundary layer near top and bottom wall.

Also vicinity to the top rotating lid, at the segment of partial heating radius (surface) the horizontal isotherms indicates dominating nature of conductive heat transfer over convection for very small thickness. However, below to that vertical isotherms line and horizontal temperature gradient induced .A zone of convective heat flow induced. Fig 10 (a) shows the behavior of Nusselt number at bottom fixed wall Nu_c, increases by increasing the partial heating radius (surface) of top lid. The Nusselt number Nu_c increases in radial direction and it is maximum at maximum radius.

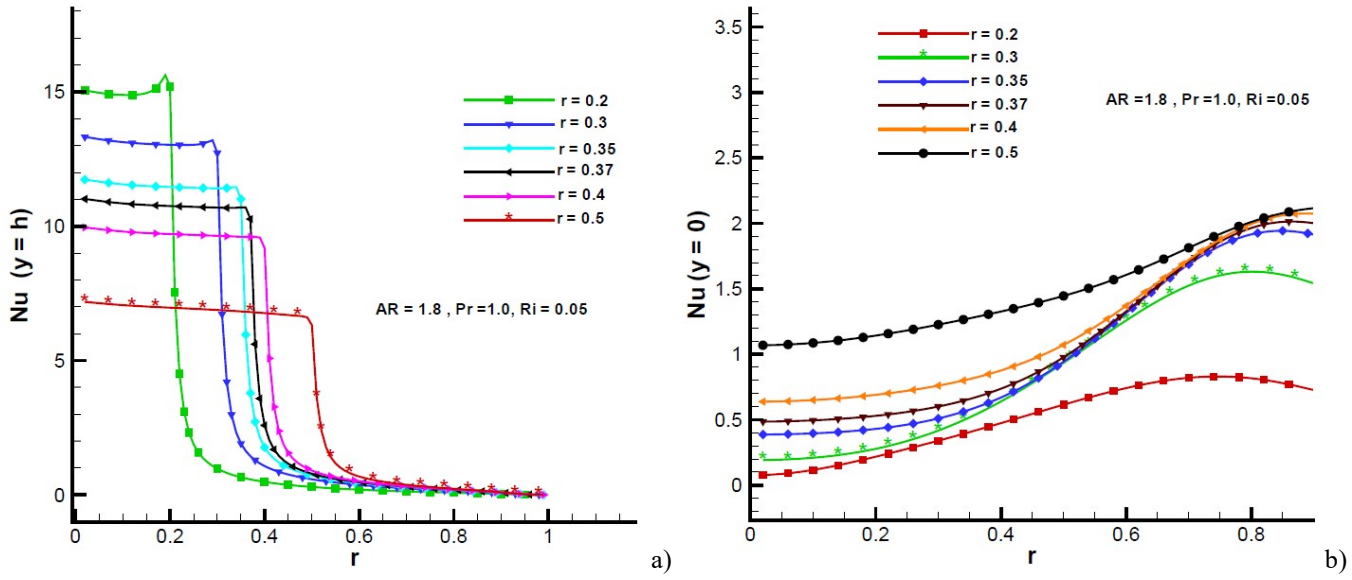

a) b)

Fig. 10 Nusselt at Re= 1500, AR =1.8,Ri=0.05, Pr =1.0.(a) r_h= 0.4 (b) r_h= 0.45(c) r_h= 0.5

Hence convective heat flow dominants the conductive part of heat transfer.However, the radial profile of Nusselt number Nu_h at top rotating lid decreases with increase in partial heating radius (surface) shown in Fig 10(b).This phenomenon shows that with increase in partial heating surface area, when heating at constant temperature gradient, constant Reynolds number, constant Prandtl number and constant Richardson number convective heat transfer vicinity to the hot rotating lid surface decreases and conductive heat transfer increases.The partial heating effects on average Nusselt number are shown in Fig 11.

The magnitude of average Nusselt numbers, vicinity to top rotating lid and bottom stationary lid, are shown in Table4. It increases with increase in partial heating surface area r_h . This indicates the increase in overall convective heat flow in axial direction. The changes in axial profile of radial, azimuthal and axial velocity components at radius r =0.2 for different surface heating radius ($0.5 \le r_h \ge 0.2$) shown in Fig 12, Fig13, and Fig 14 respectively. Remarkable changes are visible only in azimuthal and axial component of velocity. The axial profiles of azimuthal component velocity near bottom stationary lid and top rotating lid do not show any variations with increase in partial heating surface. Within the core of cavity it changes in radial direction.

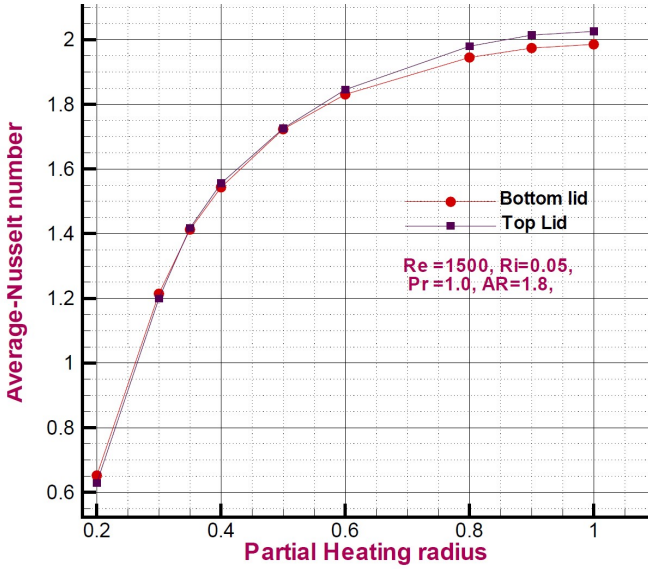

Fig. 11 Average Nusselt Number $\overline{Nu_h}$ and $\overline{Nu_C}$ vicinity to top rotating lid and bottom stationary wall

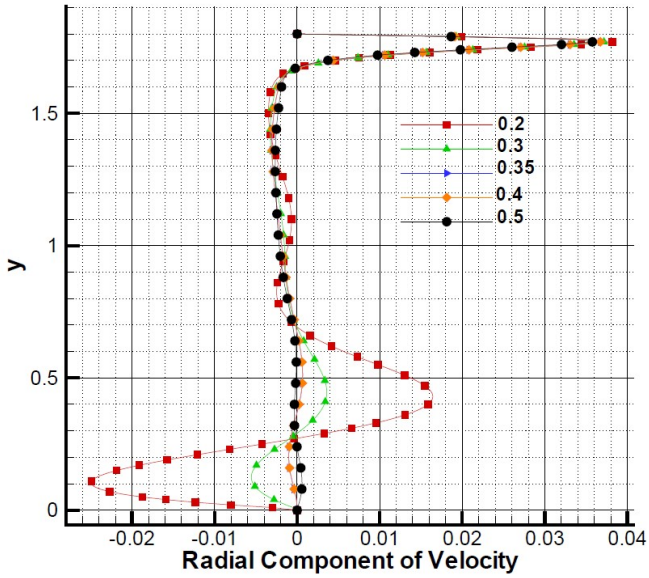

Fig. 12 Axial profile of radial component velocity at radius r =0.2 at different partial heating surface (radius = r_h =0.2, 0.3, 0.35, 0.4, 0.5)

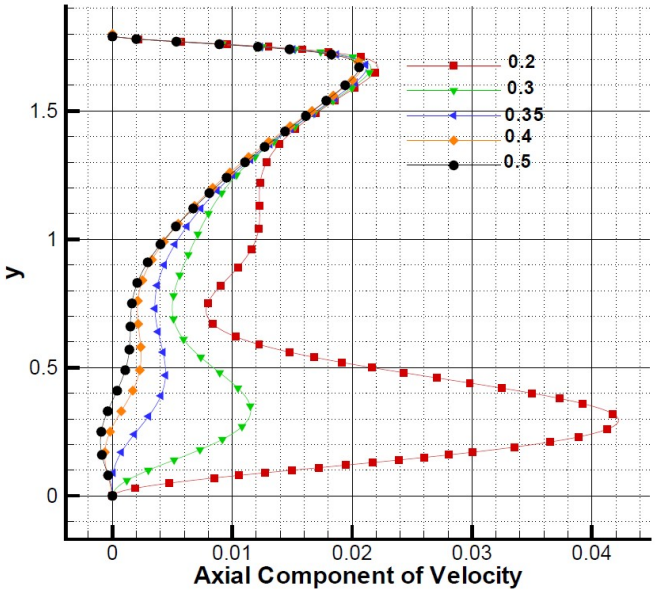

Fig. 14 Axial profile of axial component velocity at radius r =0.2 at different partial heating surface (within the plot, partial heating radius = r_h =0.2, 0.3, 0.35, 0.4, 0.5)

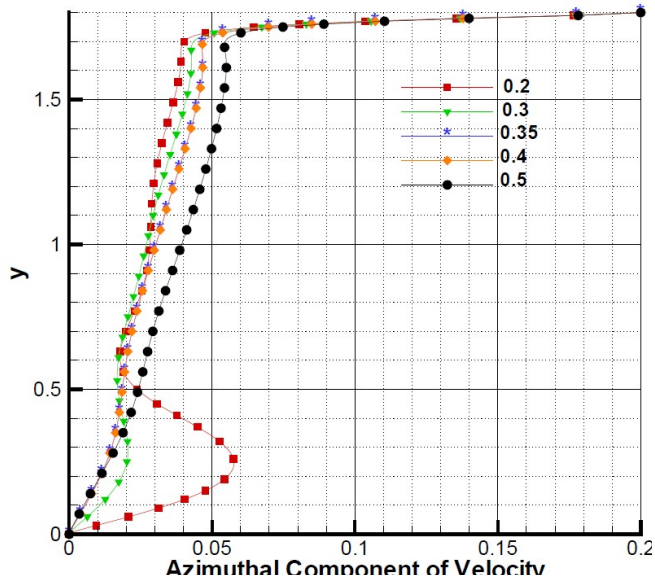

Fig. 13 Axial profile of Azimuthal component velocity at radius r =0.2 at different partial heating surface (radius = r_h =0.2, 0.3, 0.35, 0.4, 0.5)

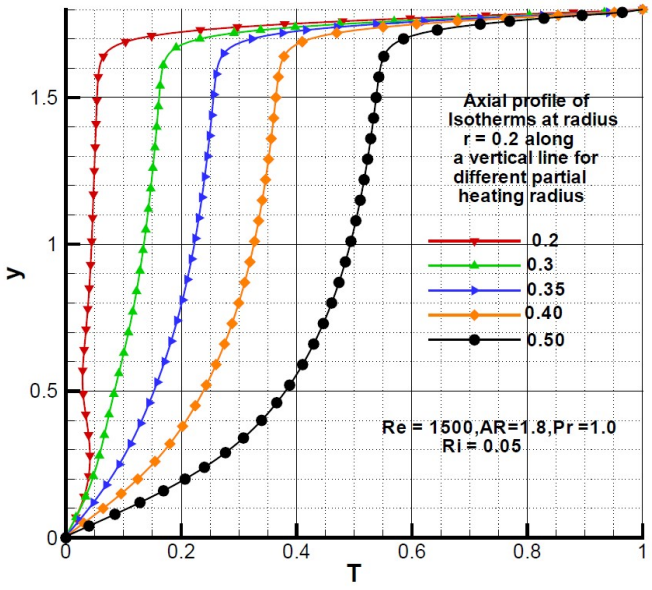

Fig. 15 Axial profile of isotherms at radius r =0.2 for different partial heating surface (within the plot, partial heating radius = r_h =0.2, 0.3, 0.35, 0.4, 0.5)

In Fig. 15 the axial profile of isotherms shows drastic variation in along the cylindrical cavity at radius r =0.2 with increase in partial heating length ($0.5 \le r_h \ge 0.2$). Also with increase in partial heating radius the variation in temperature

gradient in vertical direction vicinity to top rotating lid decreases. For $r_C = 0.2$ at radius 0.2 the axial profile of isotherm in vertical direction remains almost constant. When $r_C > 0.2$, the axial profile of isotherms in vertical direction produces temperature gradient at radius 0.2. This gradient magnifies with increase in partial heating radius as buoyancy effects enhance.

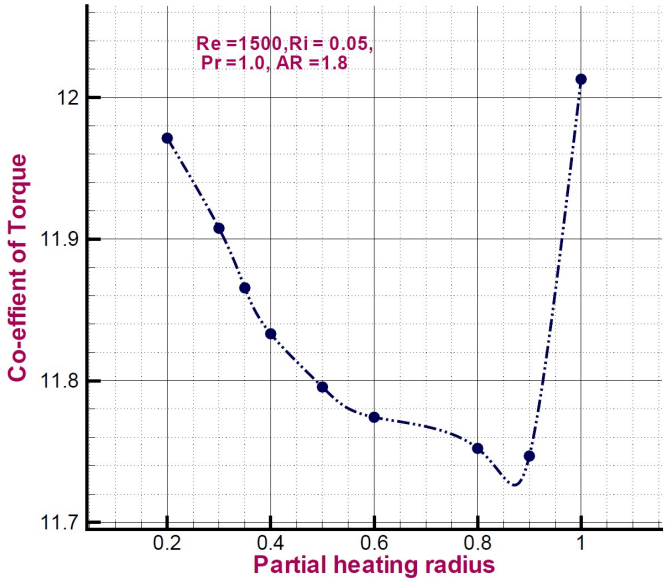

Fig. 16 Nusselt at Re= 1500, AR =1.8,Ri =0.05, Pr =1.0.(a) r_h= 0.4 (b) r_h= 0.45(c) r_h= 0.5

The coefficient of torque decreases with increase in partial heating radius vicinity to top rotating lid shown in Fig 16. At the condition $r_C = r$ (radius of partial heating = radius of top rotating lid= radius of cylindrical cavity) the coefficient of torque increases to its pick value.

The magnitude of average Nusselt numbers, vicinity to top rotating lid and bottom stationary lid, are shown in Table 4. It increases with increase in partial heating surface area r_h. This indicates the increase in overall convective heat flow in axial direction.

CONCLUSION

The study concluded that the Partial heating effects can be used as a function of vortex breakdown. It also develops different flow patterns. The increase in partial heat transfer radius changes the types of heat transfer i.e. conduction or convection .When length (area) of partial heating radius of top rotating lid increases, conductive heat transfer zone expands near to bottom cold wall. Only a small thickness of thermal boundary layer appears vicinity to partial heating surface (length).Below to that convective heat transfer prevails to most part of the cavity. The thermodynamic effects on vortex breakdown during swirling flow can be further studied for different fluid.

NOMENCLATURE

Non-dimensional numbers

Re	Reynolds number $\frac{\Omega R^2}{\nu}$
Ri	Richardson Number $\frac{g\beta(T_h - T_C)}{R\Omega^2}$
$Ny_{y=0}$	Local Nusselt number $\left.\frac{\partial T}{\partial y}\right\|_{y=0}$
$Ny_{y=h}$	Local Nusselt number $\left.\frac{\partial T}{\partial y}\right\|_{y=h}$
$\overline{Nu_h}$	Average Nusselt Number at top rotating hot lid
$\overline{Nu_C}$	Average Nusselt Number at bottom cold wall
Pr	Prandtl Number $\frac{\nu}{\alpha}$

Symbols

AR	aspect ratio = H/R
$CTtop$	Co-efficient of torque $\frac{1}{\pi}\int \left.\frac{\partial u_\theta}{\partial y}\right\|_{y=h} 2\pi r^2 dr$
H	Height of cylinder [m]
R	Radius of the cylinder[m]
r, h	Non-dimensional radius and height of cylinder
p	Non-dimensional pressure
r	Non-dimensional radius of rotating lid, cylindrical cavity and bottom stationary wall.
r_h	Non-dimensionless radius of partial heating surface of top rotating lid
r, y	Non-dimensional meridional coordinate
T	Non-dimensionless Temperature
T_h	Non-dimensional temperature at top lid
T_C	Non-dimensional temperature at bottom wall

t Non-dimensional time .

u_r, u_θ, u_y Non-dimensional velocity components in the radial azimuthally and axial directions respectively.

Greek Symbol

Ω Constant angular speed of top rotating disc
ψ Non-dimensional stream function
$\psi_{\max}$ Maximum value of stream function
$\psi_{\min}$ Minimum value of stream function
Δt Discrete time interval
Δx length of each grid element
Δy height of each grid element

Subscripts:

c Cold
h Hot
r, θ, y Radial, Axial and Azimuthal directions, respectively

REFERENCES

1. Vogel,H.U.(1968), ExperimentelleErgebnisse über die laminareStrömung in einemzylindrischenGehäusemitdarinrotierenderScheibe *(Doctoral dissertation, MPIStrömungsforschung*).
2. Pao, H. P. (1970). A numerical computation of a confined rotating flow. Journal of Applied Mechanics, 37(2), 480-487.
3. Bertelá, M., &Gori, F. (1982). Laminar flow in a cylindrical container with a rotating cover. *Journal of fluids engineering*, *104*(1), 31-39.
4. Lugt, H. J., &Haussling, H. J. (1982). Axisymmetric vortex breakdown in rotating fluid within a container. *Journal of Applied Mechanics*, *49*(4), 921-923.
5. Escudier, M. P. (1984). Observations of the flow produced in a cylindrical container by a rotating endwall. *Experiments in Fluids*, *2*(4), 189-196.
6. Lugt, H. J., &Abboud, M. (1987). Axisymmetric vortex breakdown with and without temperature effects in a container with a rotating lid. *Journal of Fluid Mechanics*, *179*, 179-200.
7. Arkadyev, A., Bar-Yoseph, P., Solan, A., &Roesner, K. G. (1993). Thermal effects on axisymmetric vortex breakdown in a spherical gap. *Physics of Fluids A: Fluid Dynamics (1989-1993)*, *5*(5), 1211-1223.
8. Lee, C. H., & Hyun, J. M. (1999). Flow of a stratified fluid in a cylinder with a rotating lid. *International journal of heat and fluid flow*, *20*(1), 26-33.
9. Kim, W. N., & Hyun, J. M. (1997). Convective heat transfer in a cylinder with a rotating lid under stable stratification. *International Journal of Heat and Fluid Flow*, *18*(4), 384-388.
10. Iwatsu, R. (2004). Flow pattern and heat transfer of swirling flows in cylindrical container with rotating top and stable temperature gradient. *International journal of heat and mass transfer*, *47*(12), 2755-2767.
11. Chen, S. (2011). Entropy generation inside disk driven rotating convectional flow. *International Journal of Thermal Sciences*, *50*(4), 626-638.
12. Chorin, A. J., A Numerical method for solving incompressible viscous flow problems, Journal of Comput. Phys., Vol 2, pp 12-26, 1967.
13. Peyret, R.&Taylor, D.(1983*)*. Computational methods for fluid flow;SprigerVerlag.
14. S.C. Dash. (2015), Incompressible confined swirling flow in a cylindrical cavity with rotating lid under the influence of axial temperature gradient or axial magnetic field, Ph. D. Dissertation, *Aerospace engineering department, IIT Kharagpur*, West Bengal, INDIA.